HHS Public Access

Author manuscript

J Drug Target. Author manuscript; available in PMC 2019 June 01.

Published in final edited form as:

J Drug Target. 2018 ; 26(5-6): 474–480. doi:10.1080/1061186X.2018.1428808.

Uric acid and the vaccine adjuvant activity of aluminum (oxy)hydroxide nanoparticles

Sachin G Thakkar[1], **Haiyue Xu**[1], **Xu Li**[1], and **Zhengrong Cui**[1,2,*]

[1]The University of Texas at Austin, College of Pharmacy, Division of Molecular Pharmaceutics and Drug Delivery, Austin, TX

[2]Inner Mongolia Medical University, Inner Mongolia Key Laboratory of Molecular Biology, Hohhot, Inner Mongolia, China

Abstract

In an effort to improve the adjuvanticity of insoluble aluminum salts, we discovered that the adjuvant activity of aluminum salt nanoparticles is significantly stronger than aluminum salt microparticles, likely related to nanoparticle's stronger ability to directly activate NLRP3 inflammasome as the nanoparticles are more efficiently taken up by phagocytic cells. Endogenous signals such as uric acid from cell damage or death caused by the cytotoxicity of aluminum salts are thought to indirectly activate inflammasome, prompting us to hypothesize that the potent adjuvant activity of aluminum salt nanoparticles is also related to their ability to stimulate uric acid production. In the present study, we prepared aluminum (oxy)hydroxide nanoparticles (~30–100 nm) and microparticles (X_{50}, 9.43 μm) and showed that intraperitoneal injection of mice with the nanoparticles, absorbed with ovalbumin, led to a significant increase in uric acid level in the peritoneal lavage, whereas the microparticles did not. The aluminum (oxy)hydroxide nanoparticles' ability to stimulate uric acid production was also confirmed in cell culture. We concluded that the stronger adjuvant activity of insoluble aluminum (oxy)hydroxide nanoparticles, relative to microparticles, may be attributed at least in part to their stronger ability to induce endogenous danger signals such as uric acid.

Keywords

Aluminum hydroxide; Nanoparticles; Microparticles; Uric acid; Vaccine adjuvant

1. Introduction

Many human vaccines contain insoluble aluminum salts such as aluminum (oxy)hydroxide and aluminum (hydroxy)phosphate as adjuvants (Kaddar, 2008, Thakkar and Cui, 2017). Although insoluble aluminum salts have been used in vaccines for decades, their exact mechanisms of action remain elusive (HogenEsch, 2002, HogenEsch, 2012). Over the years, various theories have been proposed to explain the mechanisms underlying the adjuvant activity of insoluble aluminum salts. It is clear now that the mechanisms of adjuvanticity of

[*]**Correspondence to:** Zhengrong Cui, Ph.D., The University of Texas at Austin, College of Pharmacy, Austin, TX 78712, Tel: (512) 495-4758, Fax: (512) 471-7474, zhengrong.cui@austin.utexas.edu.

aluminum salts are complex. Proposed mechanisms of immunopotentiation by aluminum salt-based adjuvants include (i) the formation of antigen depot, although the depot theory has been challenged (Marrack et al., 2009, Hutchison et al., 2012, He et al., 2015), (ii) stimulation of antigen-presenting cells such as dendritic cells (DCs) and macrophages (Mannhalter et al., 1985), (iii) complement activation (Ulanova et al., 2001), and (iv) stimulation of inflammatory and innate immune responses (Ulanova et al., 2001, HogenEsch, 2002, Wang et al., 2013, Rincon et al., 2017). In addition, there are reports showing that insoluble aluminum salts activate the intracellular pathogen pattern recognition receptor signaling pathway involving the NACHT, LRR and PYD domains-containing protein 3 (NLRP3) inflammasome by directly engaging phagocytic cells such as macrophages, and the engulfment of aluminum salt particles leads to lysosomal rupture (Eisenbarth et al., 2008, Kool et al., 2008a). Potent inflammatory cytokines such as IL-1β and IL-18 are released in response to NLRP3 activation, which direct the host responses to infection and injury (Martinon et al., 2009). Furthermore, Kool and colleagues reported that aluminum salt-based adjuvants boost adaptive immunity by inducing uric acid (Kool et al., 2008b). They showed that intraperitoneal injection of an aluminum salt (Imject Alum)-adjuvanted model vaccine into mice led to a significant increase in uric acid level in the intraperitoneal lavage, and pre-treatment of the mice with uricase, an uric aciddegrading enzyme, inhibited $CD4^+$ T cell priming (Kool et al., 2008b), suggesting an indirect pathway for insoluble aluminum salts to activate NLRP3 inflammasome (Marrack et al., 2009). Uric acid and other molecules such as high mobility group box 1 (HMGB1), ATP, heat shock proteins (HSPs), DNA, IL-1α, and filamentous actin comprise a group of substances called alarmins or danger-associated molecular patterns (DAMPs), and they were reported to be involved in immunopotentiation by aluminum salt-based adjuvants (Kool et al., 2008b, Rock et al., 2010, Marichal et al., 2011). Moreover, there were reports that DNA released by dying host cells upon treatment with aluminum salts mediates the adjuvanticity of aluminum salts (Marichal et al., 2011, McKee et al., 2013), but Noges et al. (2016) reported that contamination of DNase preparations confounds analysis of the role of host DNA in the adjuvanticity of aluminum salts (Noges et al., 2016).

Previously we and others discovered that the adjuvant activity of aluminum (oxy)hydroxide and aluminum (hydroxy)phosphate could be significantly improved by reducing the size of the particles in the aqueous suspensions of the insoluble aluminum salts from micrometer scale to nanometer scale (e.g. from 1–20 μm to ~100 nm) (Sun et al., 2013, Li et al., 2014, Ruwona et al., 2016, Li et al., 2017). We further provided evidence that the more potent adjuvant activity of the aluminum salt nanoparticles is likely related to their stronger ability in activating the NLRP3 inflammasome than aluminum salt microparticles as in cell culture, phagocytic cells (e.g. macrophages) can more effectively internalize the aluminum salt nanoparticles than microparticles, presumingly leading to increased lysosomal damage and rupture (Ruwona et al., 2016).

In an effort to further elucidate the mechanisms underlying the stronger adjuvant activity of the aluminum salt nanoparticles, relative to microparticles, we evaluated and compared aluminum (oxy)hydroxide nanoparticles (AH-NPs) and microparticles (AH-MPs) in their ability to induce uric acid production in culture and in a mouse model, hypothesizing that the AH-NPs are more potent than AH-MPs in inducing the endogenous danger signal uric

acid. Based on Kool and colleagues' findings, more uric acid is expected to be associated with a stronger immunopotentiation (Kool et al., 2008b).

2. Materials and methods

2.1 Reagents

The Aluminum Hydroxide Nanopowder/Nanoparticles (high purity, 99.9%, # US3026) were from the US Research Nanomaterials, Inc. (Houston TX). Polyvinylpyrrolidone, phosphate-buffered saline (PBS), ovalbumin (OVA), Sigma- Aldrich uric acid assay kit, MTT (3-(4,5-dimethylthiazol-2-yl)-2,5-diphenyltetrazolium bromide) reagent were from Sigma-Aldrich (St. Louis, MO). Cell culture medium, penicillin, streptomycin, and fetal bovine serum (FBS) were from Invitrogen (Carlsbad, CA). Amplex® red uric acid assay kit was from Molecular Probes/Life Technologies (Eugene, OR). Mouse J774A.1 macrophage cells (# TIB-67™) were from the American Type Culture Collection (Manassas, VA)

2.2 Preparation and characterization of aluminum (oxy)hydroxide nanoparticles (AH-NPs) and microparticles (AH-MPs)

AH-NPs and AH-MPs were prepared as described previously (Ruwona et al., 2016). Briefly, the Aluminum Hydroxide Nanopowder was slowly added into warm water while stirring. The suspension was probe-sonicated and spun at 1000 rcf for 10 min. The supernatant was probe-sonicated repeatedly and spun down again at 1000 rcf for 10 min. The resultant supernatant in suspension was stabilized by adding polyvinylpyrrolidone (1%, w/v) and used as nanoparticles (AH-NPs). The sediment was re-suspended and used as microparticles (AH-NPs) in subsequent studies.

The AH-NPs and AH-MPs were examined using an FEI Tecnai Transmission Electron Microscope (TEM) available in the Institute for Cellular and Molecular Biology (ICMB) Microscopy and Imaging Facility at The University of Texas at Austin. Carbon- coated 400-mesh grids were activated for 1–2 min. One drop of the particle suspension was deposited on the grids and incubated for 2 min at room temperature. The grids were washed with water and air-dried for 1 min. Extra water was removed using filter paper and allowed to air-dry for 15 min before observation (Li et al., 2014). The size of the particles was estimated based on randomly selected particles from the TEM micrographs. The aluminum contents in the AH-NPs and AH-MPs preparations were determined using a Varian 710-ES Inductively Coupled Plasma-Optical Emission Spectrometer (ICP-OES) in the Civil Architectural and Environmental Engineering Department at The University of Texas at Austin. XRD analysis of the AH-NPs and AH-MPs in powder was performed using an R-Axis Spider with a Cu sealed tube source with a large, image plate detector (Rigaku, The Woodlands, TX) in the Chemical Engineering Department at The University of Texas at Austin. The particles were lyophilized into powder before XRD analysis. All XRD patterns were collected with a step size of 0.01 and counting time of 1 s per step over a 2θ range of 10 to 80.

2.3 MTT assay and quantification of uric acid in cell culture medium

Mouse J774A.1 macrophage cells were grown in DMEM supplemented with 10% FBS (v/v), 100 U/mL of penicillin and 100 μg/mL of streptomycin. MTT assay was used to

determine J774A.1 cell viability after the cells (2500 cells/well) were cultured with AH-NPs or AH-MPs (aluminum content, 173 μg/well) for 72 h. Briefly, 20 μL of MTT reagent (5 mg/mL) was added to the wells and incubated at 37° C in the dark for 3–4 h. Two hundred microliters (200 μL) of dimethyl sulfoxide was added into each well and incubated for an additional 15 min to solubilize the MTT-formazan product. Absorbance was measured at 570 nm. A cell viability of greater than 90% was considered non-toxic. Triton X-100 (0.001%, v/v) was used as a positive control.

To determine uric acid production, J774A.1 cells were incubated with the AH-NPs or AH-MPs as mentioned above, and uric acid concentration in the cell culture medium was determined using a Sigma-Aldrich uric acid assay kit following the manufacturer's instructions.

2.4 Animal study

The animal study was conducted following the U.S. National Research Council Guidelines for Care and Use of Laboratory Animals. Animal protocol was approved by the Institutional Animal Care and Use Committee at The University of Texas at Austin. Female BALB/c mice (18–20 g, Charles River Laboratories, Wilmington, MA) were injected intraperitoneally (i.p.) with OVA-adsorbed AH-NPs (6 mice) or OVA-adsorbed AH-MPs (5 mice), both in a 0.9% sterile NaCl solution. The dose of aluminum was 263 μg per mouse, and the dose of OVA was 10 μg per mouse. As controls, mice were injected with a sterile 0.9% NaCl (5 mice) solution or OVA adsorbed on Alhydrogel® (aluminum, 263 μg; OVA, 10 μg). Peritoneal lavage was collected 6 h later. Uric acid level in the lavage sample was determined using the Amplex® red uric acid assay kit following the manufacturer's instructions.

2.5 Statistical analysis

Statistical analyses were completed by performing two-tailed Student's t-test for two-group analysis or one-way ANOVA followed by Tukey's post hoc analysis for multiple group comparisons (GraphPad Prism 7 software, La Jolla, CA). A p value of ≤ 0.05 (two-tail) was considered significant.

3. Results and discussion

Previously, we and others have shown that the adjuvant activity of aluminum salt nanoparticles is significantly stronger than microparticles (Sun et al., 2013, Li et al., 2014, Ruwona et al., 2016, Li et al., 2017). We further provided evidence that the stronger adjuvant activity of the aluminum salt nanoparticles are related to the nanoparticle's stronger ability to activiate NLRP3 inflammasome, likely because of the increased uptake of the nanoparticles by phagocytic cells such as macrophages, as compared to the microparticles, leading to increased lysosomal damage and rupture (Ruwona et al., 2016). Previously, Kool and colleagues provided evidence of an indirect pathway to inflammasome activation by extracellular uric acid crystals produced by damaged or dying cells caused by the cytotoxicity of aluminum salts (Kool et al., 2008b). They showed that the immunopotentiating effect of Imject™ Alum, a preparation that contains aluminum

hydroxide and magnesium hydroxide, depends on its stimulation of uric acid in a mouse model. They found a significantly increased level of uric acid in the peritoneal lavage of mice that were i.p. injected with OVA-adsorbed Imject™ Alum (1 mg aluminim hydroxide per mouse). Importantly, degradation of uric acid by pretreating mice with uricase abolished OVA-specific $CD4^+$ T cell priming, although the effect of the uricase pretreatment on specific antibody response was not reported (Kool et al., 2008b). Therefore, we hypothesize that the stronger adjuvant activity of aluminum (oxy)hydroxide nanoparticles (AH-NPs), relative to aluminum (oxy)hydroxide microparticles (AH-MPs), is also related to the difference in their ability to stimulate uric acid, and the present study was designed to test the hypothesis.

AH-MPs and AH-NPs were prepared from same aluminum (oxy)hydroxide aqueous suspension by centrifugation as described previously (Ruwona et al., 2016). Representative TEM images of the AH-NPs and AH-MPs are shown in Fig. 1A. Shown in Fig. 1B are representative particle size distribution curves of the AH-NPs and AH-MPs. The majority of the AH-NPs were below 100 nm in diameter, whereas the median diameter of the AH-MPs (i.e., X_{50}) was 9.43 μm, with X_{10} and X_{90} values of 1.69 μm and 17.74 μm respectively (Fig. 1B). XRD analysis showed that the AH-NPs and AH-MPs have identical characteristic peaks, indicating that they have similar compositions and crystallinities (Fig. 1C). Characterisities (Fig. 1C). Characteristic peaks of boehmite (aluminum oxyhydroxide (AlOOH)), based on the XRD spectra of the Joint Committee on Powder Diffraction Standards (PDF No. 00–021-1307), are labeled for both samples. The particles were mainly amorphous due to the huge characteristic peak in the 2Θ range of 10–25, but they also contain some crystalline boehmite (Figure 1C) (Li et al., 2017).

To test whether the AH-NPs and AH-MPs are different in their abilities to induce uric acid production by cells in culture, J774A.1 mouse macrophages were incubated with AH-NPs or AH-MPs for 72 h, and uric acid levels in cell culture medium were measured. The macrophage cell line was chosen due to their known ability to engulf particles, although the damage or death of other cells induced by aluminum salts is expected to release the danger signal uric acid as well. As shown in Fig 2A, AH-NPs induced uric acid production, whereas the same concentration of AH-MPs did not. Fig. 2B shows the cytotoxicities of AH-NPs and AH-MPs to J774A.1 cells after 72 h of incubation at the same concetration as in Fig. 2A. It appears that the AH-NPs induced cell death, whereas the AH-MPs at the same aluminum concentration did not cause any significant cell death (i.e., 71% vs. 100% survival, $p < 0.0001$). Cell death or damage causes the release of the endogeneous danger signals such as uric acid, explaining why incubation of J774A.1 cells with AH-NPs caused the release of uric acid in cell culture medium, but incubation of same number of cells with the AH-MPs at the same aluminum concentration did not (Fig. 2A). It is possible that at higher concentrations and a prolonged incubation time period, the AH-MPs may be able to induce cell damage or death and thus uric acid release.

To evaluate and compare the AH-NPs and AH-MPs on their abilities to induce uric acid production *in vivo,* AH-NPs and AH-MPs were surface-adsorbed with OVA as a model antigen because for immunization, aluminum salts are not injected without an antigen *in vivo.* Kool and colleagues injected mice with Imject™ Alum adsorbed with OVA in their

study leading to the discovery that aluminum salt adjuvants boost adaptive immunity by inducing uric acid in a mouse model (Kool et al., 2008b). As shown in Fig. 2C, i.p. injection of BALB/c mice with OVA-adsorbed AH-NPs increased uric acid level in the peritoneal lavage of mice, as compared to that in mice i.p. injected with normal saline. However, i.p. injection of OVA-adsorbed AH-MPs did not increase uric acid production as compared to i.p. injection of normal saline (Fig. 2C), indicating that the potent vaccine adjuvant activity of the AH-NPs may be at least in part due to their stronger ability to induce uric acid.

It was unexpected, however, that our AH-MPs at the concentration or dose tested did not cause significant uric acid release in cell culture and in the mouse model (Fig. 2A, C). Imject™ Alum, which contains mainly microparticles (X_{10}, 0.96 μm; X_{50}, 3.24 μm; and X_{90}, 11.64 μm, Fig. 3A), were reported to induce significant local uric acid production after OVA-adsorbed Imject™ Alum was i.p. injected into mice (Kool et al., 2008b). Of course, the dose the Imject™ Alum in Kool et al's study was 1 mg per mouse (i.e. 1 mg aluminum hydroxide or 0.346 mg aluminum), whereas the dose of aluminum in the present study was 0.263 mg per mouse. Moreover, our AH-MPs (i.e., X_{10}, 1.69 μm; X_{50}, 943 μm; and X_{90}, 17–74 μm, Fig. 1(A)) were generally larger than the particles in the Imject™ Alum (e.g. the X_{50} is ~3-fold larger). Differences in the composition, particle size and size distribution, and dose between the Imject™ Alum and our AH-MPs may be responsible for their ability, or lack of ability, to induce uric acid release.

In fact, we also tested Alhydrogel®'s ability to induce uric acid release *in vivo.* Intraperitoneal injection of mice with Alhydrogel® (i.e., X_{10}, 0.67 μm; X_{50}, 1.67 μm; and X_{90}, 29.21 μm, Fig. 3B) at an aluminum dose identical to our AH-MPs, and adsorbed with OVA, significantly increased the uric acid level in the peritoneal lavage of the mice, as compared to injection of normal saline (Fig. 3C). Alhydrogel® and our AH-MPs are both mainly aluminum oxyhydroxide in composition, although Alhydrogel® has moderately high crystallinity (Li et al., 2017), whereas our AH-MPs are mainly amorphous (Fig. 1C) (Li et al., 2017). Therefore, it is likely that the particle size and size distribution of aluminum salts significantly affect their ability to induce uric acid production. It is also possible that the smaller aluminum salt particles in Alhydrogel® and Imject™ Alum, although not as small as the particles in our AH-NPs, can effectively induce uric acid production, whereas those relatively larger aluminum salts, especially the very larger ones in our AH-MPs (i.e. X_{50} = 9.43 μm), cannot. Very large aluminum salt particles such as the ones with a diameter ≥ 10 μm may be too large for cells to readily engulf them, preventing them from causing cell damage or death and inducing uric acid production. The reported average size of the rat alveolar macrophages is around 13 μm (Haley et al., 1991, Sebring and Lehnert, 1992, Krombach et al., 1997). We have measured the size of the J774A.1 mouse macrophage cells under microscope and found it to be 16.90 ± 2.47 μm (n = 50 cells). There are reports of macrophage uptake of particles larger than themselves, but the majority of the particles in our AH-MPs may be too large to be effectively taken up by mouse DCs or macrophages. Flach et al. (2011) even reported that mouse DC2.4 cells and human DCs differentiated from THP-1 cells did not internalize aluminum salt particles of ~5 μm (Flach et al., 2011). Instead, those particles induced abortive phagocytosis (Flach et al., 2011). Therefore, it is not unreasonable to hypothesize that the mechanisms by which smaller aluminum salt particles and larger ones potentiate immune responses may be different (e.g. smaller vs

larger than 4 μm (Fig. 3D)). It is possible that uric acid release may play a more important role in the adjuvant activity of smaller aluminum salt particles than the larger particles in traditional aluminum salt adjuvant such as Alhydrogel®. Of course, it is possible that large aluminum salt particles at higher concentrations and prolonged incubation time may cause cell damage and death and could in turn induce uric acid production as well.

In conclusion, the potent adjuvant activity of the aluminum (oxy)hydroxide nanoparticles is likely related to them being more effective than large aluminum (oxy)hydroxide microparticles in inducing endogenous danger signals such as uric acid. In traditional insoluble aluminum salt-based vaccine adjuvants, the mechanisms by which the relatively smaller particles potentiate immune responses may be different from the relatively larger ones.

Acknowledgments

This work was supported in part by the U.S. National Institute of Allergy and Infectious Diseases (AI105789 to ZC), the Alfred and Dorothy Mannino Fellowship in Pharmacy at UT Austin (to ZC), and The University of Texas at Austin Graduate School Dean's Fellowship (to SGT). ZC is also supported by the National Natural Science Foundation of China (81460454) and the Inner Mongolia Natural Science Fund (2014ZD05). The authors would like to thank Dr. Hugh Smyth at the UT Austin for kindly allowing us to use the Sympatec Helos laser diffraction instrument available in his lab.

References

Eisenbarth SC, Colegio OR, O'connor W, Sutterwala FS & Flavell RA, 2008 Crucial role for the Nalp3 inflammasome in the immunostimulatory properties of aluminium adjuvants. Nature, 453, 1122–1126. [PubMed: 18496530]

Flach TL, Ng G, Hari A, Desrosiers MD, Zhang P, Ward SM, Seamone ME, Vilaysane A, Mucsi AD, Fong Y, Prenner E, Ling CC, Tschopp J, Muruve DA, Amrein MW & Shi Y, 2011 Alum interaction with dendritic cell membrane lipids is essential for its adjuvanticity. Nat Med, 17, 479–87. [PubMed: 21399646]

Haley PJ, Muggenburg BA, Weissman DN & Bice DE, 1991 Comparative morphology and morphometry of alveolar macrophages from six species. Am J Anat, 191, 401–7. [PubMed: 1951138]

He P, Zou Y & Hu Z, 2015 Advances in aluminum hydroxide-based adjuvant research and its mechanism. Human vaccines & immunotherapeutics, 11, 477–488. [PubMed: 25692535]

Hogenesch H, 2002 Mechanisms of stimulation of the immune response by aluminum adjuvants. Vaccine, 20, S34–S39. [PubMed: 12184362]

Hogenesch H, 2012 Mechanism of immunopotentiation and safety of aluminum adjuvants. Frontiers in immunology, 3.

Hutchison S, Benson RA, Gibson VB, Pollock AH, Garside P & Brewer JM, 2012 Antigen depot is not required for alum adjuvanticity. FASEB J, 26, 1272–9. [PubMed: 22106367]

Kaddar M, 2008 *Global vaccine market* [online]. World Health Organization. Available from: http://www.who.int/influenza_vaccines_plan/resources/session_10_kaddar.pdf?ua=1&ua=1 [Accessed Access Date

Kool M, Petrilli V, De Smedt T, Rolaz A, Hammad H, Van Nimwegen M, Bergen IM, Castillo R, Lambrecht BN & Tschopp J, 2008a Cutting edge: alum adjuvant stimulates inflammatory dendritic cells through activation of the NALP3 inflammasome. The Journal of Immunology, 181, 3755–3759. [PubMed: 18768827]

Kool M, Soullie T, Van Nimwegen M, Willart MA, Muskens F, Jung S, Hoogsteden HC, Hammad H & Lambrecht BN, 2008b Alum adjuvant boosts adaptive immunity by inducing uric acid and activating inflammatory dendritic cells. J Exp Med, 205, 869–82. [PubMed: 18362170]

Krombach F, Munzing S, Allmeling AM, Gerlach JT, Behr J & Dorger M, 1997 Cell size of alveolar macrophages: an interspecies comparison. Environ Health Perspect, 105 Suppl 5, 1261–3. [PubMed: 9400735]

Li X, Aldayel AM & Cui Z, 2014 Aluminum hydroxide nanoparticles show a stronger vaccine adjuvant activity than traditional aluminum hydroxide microparticles. J Control Release, 173, 148–57. [PubMed: 24188959]

Li X, Hufnagel S, Xu H, Valdes SA, Thakkar SG, Cui Z & Celio H, 2017 Aluminum (Oxy)Hydroxide Nanosticks Synthesized in Bicontinuous Reverse Microemulsion Have Potent Vaccine Adjuvant Activity. ACS Appl Mater Interfaces, 9, 22893–22901. [PubMed: 28621928]

Mannhalter JW, Neychev HO, Zlabinger GJ, Ahmad R & Eibl MM, 1985 Modulation of the human immune response by the non-toxic and non-pyrogenic adjuvant aluminium hydroxide: effect on antigen uptake and antigen presentation. Clin Exp Immunol, 61, 143–51. [PubMed: 3876178]

Marichal T, Ohata K, Bedoret D, Mesnil C, Sabatel C, Kobiyama K, Lekeux P, Coban C, Akira S, Ishii KJ, Bureau F & Desmet CJ, 2011 DNA released from dying host cells mediates aluminum adjuvant activity. Nat Med, 17, 996–1002. [PubMed: 21765404]

Marrack P, Mckee AS & Munks MW, 2009 Towards an understanding of the adjuvant action of aluminium. Nat Rev Immunol, 9, 287–93. [PubMed: 19247370]

Martinon F, Mayor A & Tschopp J, 2009 The inflammasomes: guardians of the body. Annu Rev Immunol, 27, 229–65. [PubMed: 19302040]

Mckee AS, Burchill MA, Munks MW, Jin L, Kappler JW, Friedman RS, Jacobelli J & Marrack P, 2013 Host DNA released in response to aluminum adjuvant enhances MHC class II-mediated antigen presentation and prolongs CD4 T-cell interactions with dendritic cells. Proc Natl Acad Sci U S A, 110, E1122–31. [PubMed: 23447566]

Noges LE, White J, Cambier JC, Kappler JW & Marrack P, 2016 Contamination of DNase Preparations Confounds Analysis of the Role of DNA in Alum-Adjuvanted Vaccines. J Immunol, 197, 1221–30. [PubMed: 27357147]

Rincon JC, Cuenca AL, Raymond SL, Mathias B, Nacionales DC, Ungaro R, Efron PA, Wynn JL, Moldawer LL & Larson SD, 2017 Adjuvant pretreatment with alum protects neonatal mice in sepsis through myeloid cell activation. Clin Exp Immunol.

Rock KL, Latz E, Ontiveros F & Kono H, 2010 The sterile inflammatory response. Annu Rev Immunol, 28, 321–42. [PubMed: 20307211]

Ruwona TB, Xu H, Li X, Taylor AN, Shi YC & Cui Z, 2016 Toward understanding the mechanism underlying the strong adjuvant activity of aluminum salt nanoparticles. Vaccine, 34, 3059–67. [PubMed: 27155490]

Sebring RJ & Lehnert BE, 1992 Morphometric comparisons of rat alveolar macrophages, pulmonary interstitial macrophages, and blood monocytes. Exp Lung Res, 18, 479–96. [PubMed: 1516568]

Sun B, Ji Z, Liao YP, Wang M, Wang X, Dong J, Chang CH, Li R, Zhang H, Nel AE & Xia T, 2013 Engineering an effective immune adjuvant by designed control of shape and crystallinity of aluminum oxyhydroxide nanoparticles. ACS Nano, 7, 10834–49. [PubMed: 24261790]

Thakkar SG & Cui Z, 2017 Methods to Prepare Aluminum Salt-Adjuvanted Vaccines *In* Fox CB (ed.) Vaccine Adjuvants: Methods and Protocols. Springer New York, 181–199.

Ulanova M, Tarkowski A, Hahn-Zoric M & Hanson LA, 2001 The Common vaccine adjuvant aluminum hydroxide up-regulates accessory properties of human monocytes via an interleukin- 4-dependent mechanism. Infect Immun, 69, 1151–9. [PubMed: 11160013]

Wang XY, Yao X, Wan YM, Wang B, Xu JQ & Wen YM, 2013 Responses to multiple injections with alum alone compared to injections with alum adsorbed to proteins in mice. Immunol Lett, 149, 88–92. [PubMed: 23183095]

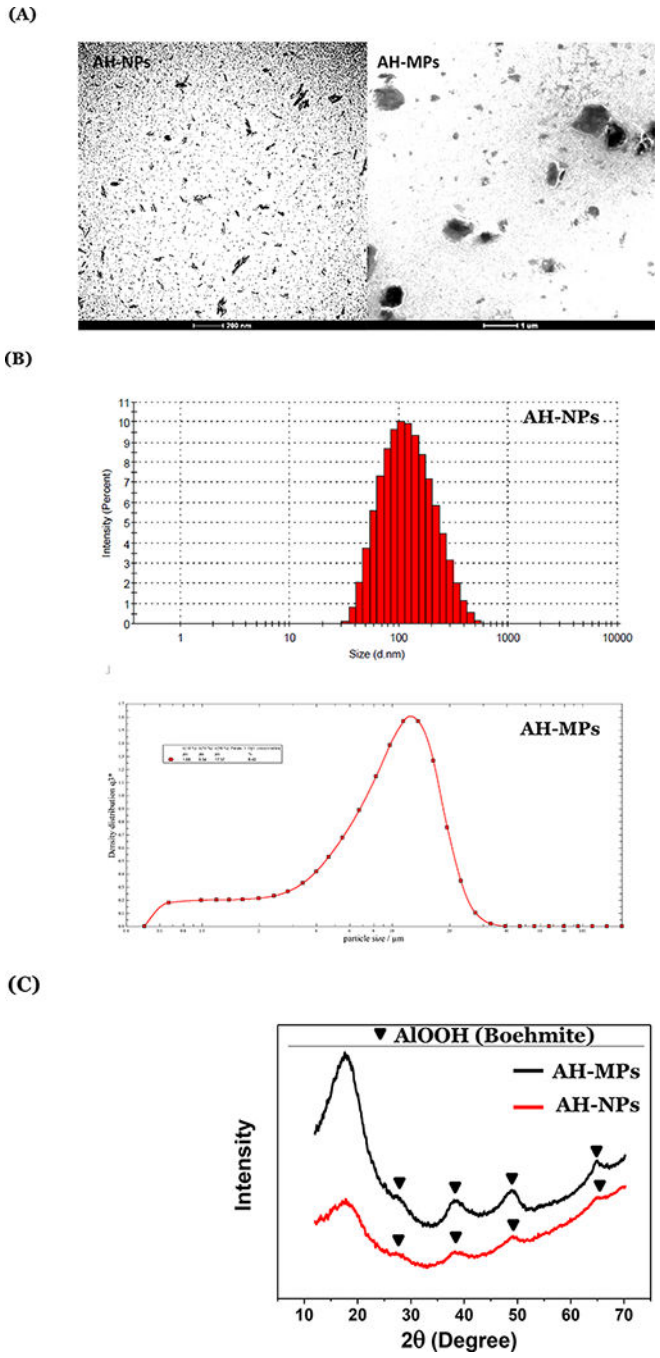

Figure 1:

Physicochemical characterization of aluminum (oxy)hydroxide nanoparticles and microparticles. **(A)** Representative TEM images of AH-NPs and AH-MPs. **(B)** Representative particle size and size distribution profiles of AH-NPs and AH-MPs as determined using dynamic light scattering and laser diffraction, respectively. **(C)** XRD patterns of the AH-MPs and AH-NPs.

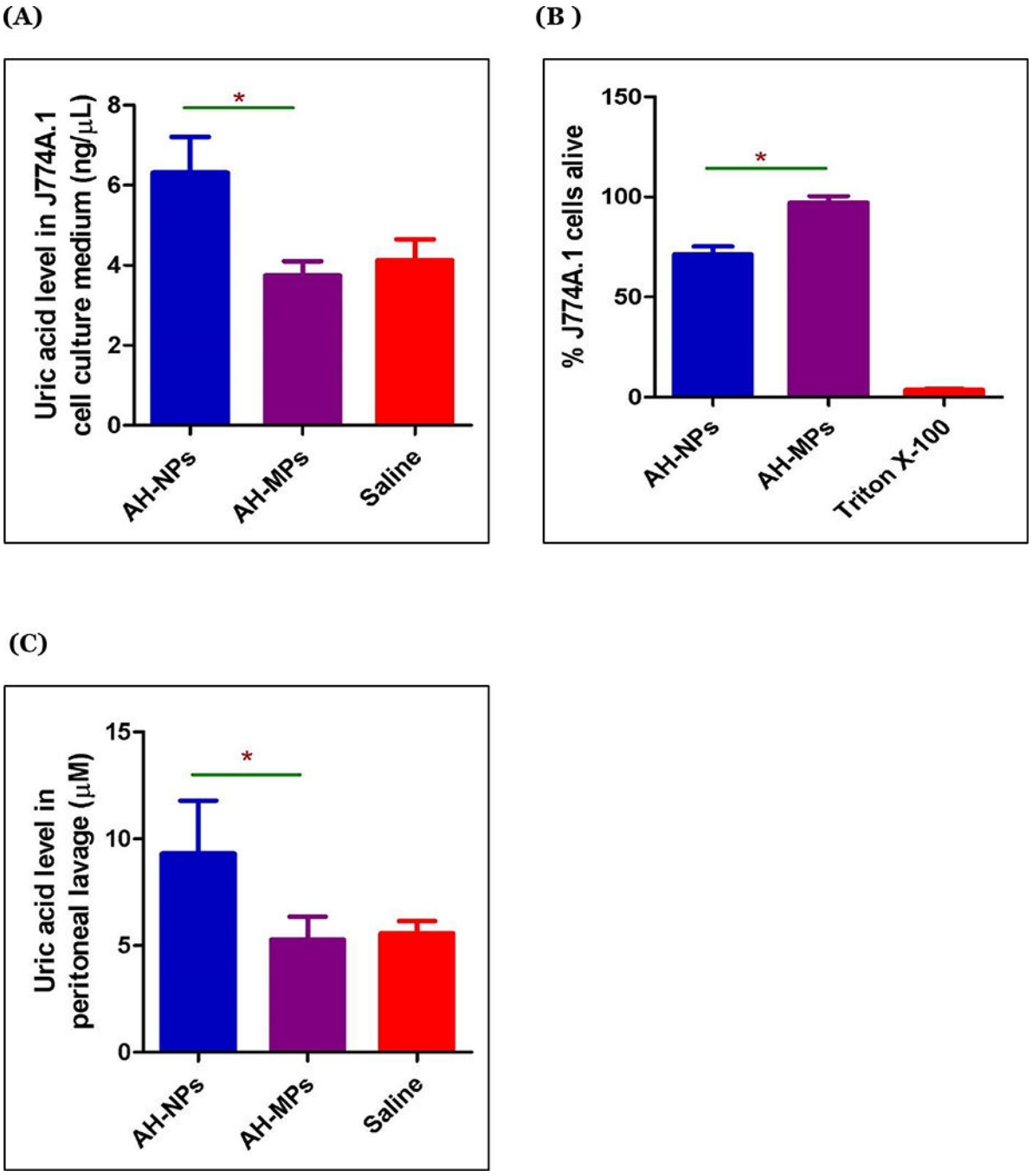

Figure 2:

Cytotoxicity and induction of uric acid by AH-NPs and AH-MPs. **(A)** J774A.1 cells were incubated with AH-NPs or AH-MPs for 72 h, and the uric acid level in culture medium was determined. Data shown are mean ± SEM ($n = 5 – 6$). * $p < 0.001$ vs AH-MPs. **(B)** J774A.1 cells were incubated with AH-NPs or AH-MPs for 72 h, and cell viability was measured. Triton X-100 was used as a positive control (* $p < 0.0001$, vs. AH-MPs). (In A-B, the number of J774A.1 cells were 2500 cells/well, and the aluminum concentration was 173 μg/well. **(C)** Uric acid levels in the peritoneal lavage of in BALB/c mice intraperitoneally

injected with AH-NPs or AH-MPs. Mice were i.p. injected with AH-NPs, AH-MPs, or normal saline, and after 6 h, the uric acid level was measured in the peritoneal lavage. AH-NPs and AH-MPs were surface-adsorbed with OVA (Aluminum, 263 μg/mouse; OVA 10 μg/mouse). Data shown are mean ± SEM ($n = 5 – 6$). * $p < 0.005$ vs. AH-MPs.

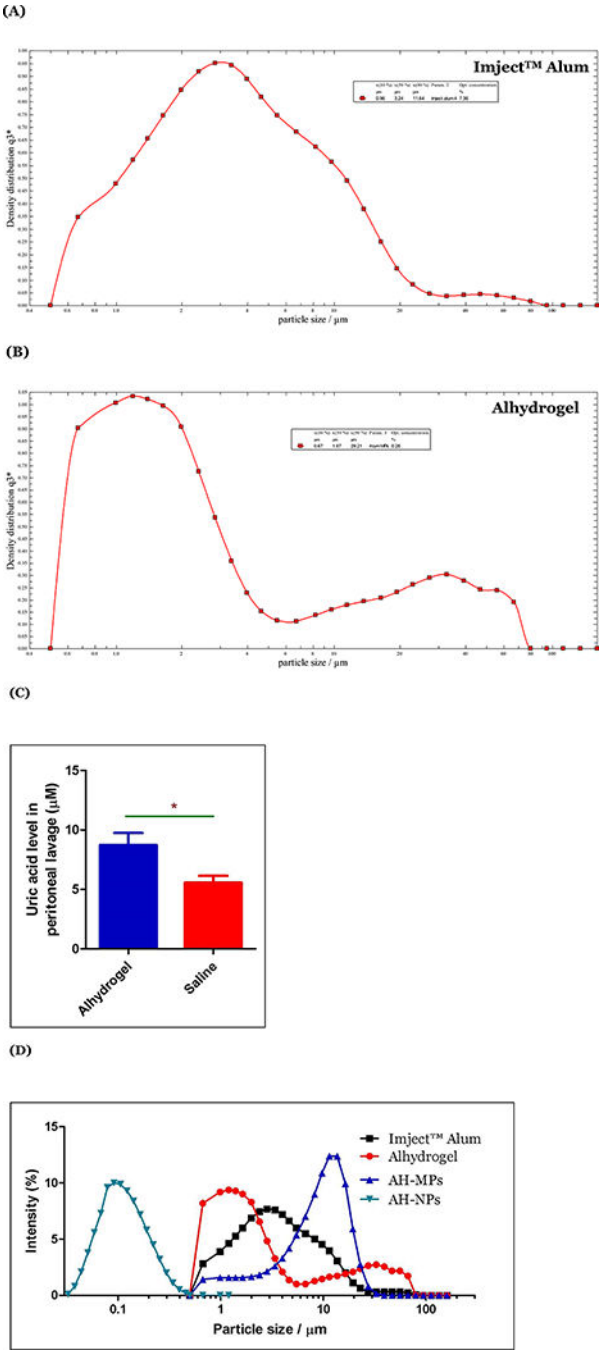

Figure 3:

(A-B) Representative particle size and size distribution profiles of Alhydrogel® (A) and Imject™ Alum (B), respectively, as determined by laser diffraction. **(C)** Uric acid induction by Alhydrogel®. BALB/c mice were i.p. injected with OVA- adsorbed Alhydrogel (Aluminum, 263 µg/mouse; OVA 10 µg/mouse) or normal saline. Uric acid level was determined in the peritoneal lavage after 6 h. Data shown are mean ± SEM (n = 5). * p <

0.0005 vs. normal saline. **(D)** An overlay of the particle size distribution curves of AH-NPs, AH-MPs, Imject™ Alum, and Alhydrogel®.